Photoreversible Hydrogen Migration System in a Solid Argon Matrix Formed by the Reaction of Methyl Fluoride with Laser-Ablated Titanium Atoms

Han-Gook Cho and Lester Andrews*

Department of Chemistry, University of Virginia, P.O. Box 400319, Charlottesville, Virginia 22904-4319

Received: April 13, 2004; In Final Form: May 24, 2004

The photoreversible system of titanium methylidene and methyltitanium fluoride complexes has been formed by the reaction of methyl fluoride and laser-ablated Ti atoms and isolated in a solid argon matrix. There are two major groups of absorptions based on broad-band irradiation and annealing behavior. The increase of group I is accompanied by the decrease of group II on photolysis with UV light (240 nm $< \lambda <$ 380 nm) and the reverse with visible light ($\lambda >$ 530 nm). The methylidene CH_2═TiHF and methyltitanium fluoride CH_3−TiF are responsible for these absorptions, and the photochemical interconversion occurs via α-H migration between carbon and titanium atoms. The methylidene complex appears to be stabilized by an agostic hydrogen interaction. Absorptions for the higher coordinated $(CH_3)_2TiF_2$ complex are observed to increase on UV irradiation and on annealing where CH_3TiF spontaneously adds CH_3F.

Introduction

Since the first discovery of the high oxidation state transition-metal complexes containing a multiple metal−carbon bond in the 1970s,[1] numerous studies have been carried out for high oxidation state alkylidenes (M═CR_1R_2) and alkylidynes (M≡CR). They are typically prepared by intramolecular α-hydrogen elimination from a bis(alkyl) precursor and are well-known for the catalytic activities of the complexes to metathesis of alkenes, alkynes, and cyclic compounds.[2] The transition-metal alkylidene complexes have not only provided a wealth of information for the nature of metal coordination chemistry but also have been industrially important as the most important metathesis polymerization catalysts.[1−3] Titanium alkylidene complexes have been proposed as intermediates in a variety of reactions, but stable alkylidene complexes of group 4 metals are rare. An example is the neopentylidene complex stabilized by PMe_3, which contains a relatively short Ti═C bond (1.884 Å).[4]

Transition-metal methylidenes derived from simple halomethanes, the simplest form of alkylidene complexes, are an ideal model system to study the effects of ligands and substituent modifications, but they are inherently unstable due to the lack of stabilizing resonance structures. Recently, reaction of laser-ablated zirconium atoms and methyl fluoride in excess argon during condensation has been carried out in this laboratory, and CH_2═ZrHF in its lowest singlet and triplet states has been identified for the first time in the infrared spectrum along with the Grignard-type molecule CH_3−ZrF.[5] Interestingly enough, the methylidene in the singlet and triplet states frozen in a solid matrix consists of a persistent photoreversible system via intersystem crossing, and CH_3−ZrF rearranges to CH_2═ZrHF on UV photolysis.

It is therefore intriguing to determine whether titanium, another group 4 transition metal, can form similar methyl metal fluoride and methylidene complexes and even a photoreversible system. Titanium is often very reactive: Ti reacts readily with O_2, N_2, and H_2 to form various products.[6−8] Recently Manceron et al. reported an infrared matrix isolation study of reaction products of titanium atoms with ethylene.[9] They identified two groups of absorption bands based upon differences in relative product yields on electronic excitation of Ti with visible light irradiation. The two groups of absorptions were assigned to two oxidative reaction products: a C−H insertion and a metallacyclic dihydride species. Finally, if CH_3TiF can be formed, what about $(CH_3)_2TiF_2$? The $(CH_3)_2TiCl_2$ analogue has been investigated in part because of the possibility of agostic hydrogen behavior.[10]

The transition-metal methylidenes derived from simple halomethanes have been the subject of theoretical studies for molecular structure and reactivity. Hehre et al. investigated variation in the bond lengths and hybridization in formation of group 4 transition-metal methylidenes.[11] Cundari and Gordon examined the geometry, vibrational characteristics, and electronic structures of the possible methylidene complexes from halomethanes and groups 4 and 5 transition-metal atoms.[12] More recently Siegbahn and Bloomberg studied C−H activation by transition-metal atoms and the effects of halide substitution.[13]

Jacox and Milligan reported the infrared spectra of methyl fluoride fragments (e.g., CF, HCF, and H_2CF radicals) formed by vacuum UV photolysis of methyl fluoride and isolated in a solid argon matrix.[14] Other radicals and ions related to methyl fluoride and reactions of halomethanes with alkali metals have also been studied.[15−21] Finally, C−H insertion by laser-ablated metal atoms has been observed in various systems in our laboratory.[22−24]

In this investigation, laser-ablated Ti atoms were reacted with methyl fluoride diluted in argon, and the products captured in a solid argon matrix were investigated by means of infrared spectroscopy. Results show five groups of absorptions on the basis of the behaviors upon photolysis and annealing, and interestingly enough, two of them define a persistent photoreversible system in the matrix. Several additional infrared absorptions are believed to arise from electronic transitions. The vibrational characteristics of the product absorptions are confirmed by isotopic substitution and density functional theory calculations.

* Author for correspondence. E-mail: lsa@virginia.edu.

10.1021/jp0483775 CCC: $27.50
Published on Web 07/07/2004

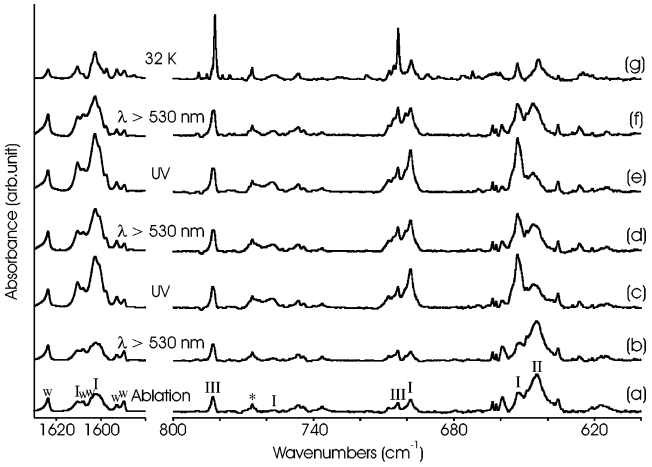

Figure 1. IR spectra in the regions of 1580−1630 and 600−800 cm^{-1} for laser-ablated Ti atoms co-deposited with Ar/CH_3F at 7 K. (a) Ti + 0.2% CH_3F in Ar co-deposited for 1 h, (b) after broad-band photolysis with a filter (λ > 530 nm) for 30 min, (c) after broad-band photolysis with a UV transmitting filter (240 nm < λ < 380 nm) for 10 min, (d) after broad-band photolysis with a filter (λ > 530 nm) for 30 mim, (e) after broad-band photolysis with a UV transmitting filter (240 nm < λ < 380 nm) for 10 min, (f) after broad-band photolysis with a filter (λ > 530 nm) for 60 min, and (g) after annealing to 32 K. "I", "II", or "III" stands for the product band group. The absorptions of water impurity and TiN_2 are marked with "w" and "*", respectively.

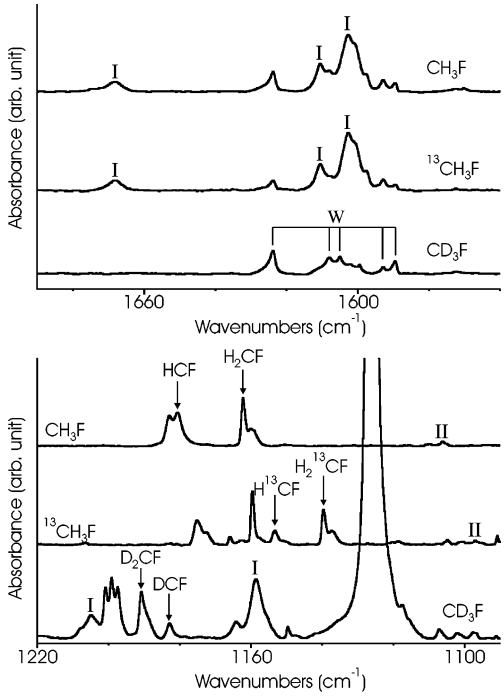

Figure 2. IR spectra in the regions of 1510−1580 and 1070−1140 cm^{-1} after UV (240 nm < λ < 380 nm) photolysis following co-deposition of laser-ablated Ti atoms with methyl fluoride isotopomers diluted in Ar at 7 K. The product absorptions are identified with "I" or "II" depending on the group they belong to. The absorptions of methyl fluoride fragments are also identified with the name of the species. Water absorptions are indicated as well.

Experimental and Computational Methods

Laser-ablated titanium atoms (Johnson-Matthey) were reacted with CH_3F (Matheson), CD_3F (synthesized from CD_3Br and HgF_2),[16] and $^{13}CH_3F$ (MSD Isotopes, 99%) in excess argon during condensation at 7 K using a closed-cycle He refrigerator (Air Products HC-2). The methods were previously described in detail elsewhere.[25−28] Concentrations of gas mixtures, typically 0.2% in argon, ranged between 0.1 and 0.5%. After reaction, infrared spectra were recorded at a resolution of 0.5 cm^{-1} using a Nicolet 550 spectrometer with an HgCdTe detector. Samples were later irradiated by a combination of optical filters and a mercury arc lamp (175 W, quartz envelope) and annealed, and more spectra were recorded.

Complementary density functional theory (DFT) calculations were carried out using the Gaussian 98 package,[29] B3LYP density functional, 6-311+G(2d,p) basis sets for C, H, F, and SDD pseudopotential, and basis set for Ti (18 electron core) to provide a consistent set of vibrational frequencies for the anticipated reaction products. Geometries were fully relaxed during optimization, and the optimized geometry was confirmed via vibrational analysis. All the vibrational frequencies were calculated analytically. In calculation of the binding energy of a metal complex, the zero-point energy is included. For comparison, calculations were also done using the all-electron basis on titanium: The frequencies were slightly lower for both major product molecules.

Results and Discussion

Figure 1 shows the IR spectra in the regions of 1580−1630 and 600−800 cm^{-1} for laser-ablated Ti atoms co-deposited with Ar/CH_3F at 7 K and their variation upon irradiation and annealing. In the region of 1580−1630 cm^{-1}, product absorptions are found at 1602.8 and 1610.6 cm^{-1}. Irradiation with a broad-band Hg lamp and a filter (λ > 530 nm), following the co-deposition, leads to a slight decrease of the absorptions at 1602.8 and 1610.6 cm^{-1}, and so do following irradiations with visible light (λ > 470 nm, λ > 420 nm, and λ > 380 nm). On the other hand, UV (240 nm < λ < 380 nm) photolysis brings a dramatic increase of the absorptions. In the following photolysis with visible light (λ > 530 nm), the absorptions decrease but they increase again on the next UV photolysis reaching 0.021 and 0.010 absorbance, respectively. Further photolysis with visible light (λ > 530 nm) weakens the absorptions again.

As shown in Figure 2, ^{13}C substitution leads to negligible shifts in the frequency of product absorptions in the region of 1580−1630 cm^{-1}, whereas deuteration results in large shifts (444−446 cm^{-1}) (H/D isotopic frequency ratio of 1.383), indicating that they are Ti−H stretching absorptions. In earlier studies, the hydrogen stretching absorptions of titanium hydrides are also observed in the same frequency region.[8,9] The hydrogen stretching absorptions most probably arise from the same reaction product, based on the fact that the absorptions show the same behavior in photolysis and annealing.

Similar dramatic variations of absorption intensities on photolysis occur in the 600−800 cm^{-1} region and accompany the variations in the 1580−1630 cm^{-1} absorptions, as shown in Figures 1 and 3. Particularly the strong absorption at about 646.3 cm^{-1} weakens considerably on UV photolysis, while the neighboring absorption at 698.6 cm^{-1}, along with the absorptions at 652.8 and 757.8 cm^{-1}, increases significantly. Subsequent photolysis with visible light (λ > 530 nm) leads to the opposite result. It is noteworthy that this photoreversible system is persistent. The same variations in absorption intensities are observed repeatedly in the following cycles of irradiation with UV and visible light without noticeable decrease in the absorption intensities: The total intensity of the absorptions at 646 and 698 cm^{-1} remains essentially unchanged during the experiments.

Evidently the efficiency of UV photolysis is much higher than photolysis with visible light. More than 6 times longer visible (λ > 530 nm) irradiation is necessary to reverse the

TABLE 1: Frequencies of Observed Product Absorptions[a]

group	CH_3F	CD_3F	$^{13}CH_3F$	
I	1610.6, *1602.8*	1164.2, *1158.6*	1610.6, *1602.8*	
	757.8	644.9	748.8	
	698.6	702.6	692.0	
	652.8	522.1	646.6	
II	1109.8, *1105.7*	871.1	1107.7, *1096.9*	
	646.3	642.3	643.3	
	507.9, *504.3*	452.4, 450.9	498.3, *494.7*	
III	1385.2	1010.9	1381.9	
	1378.4		1375.2	
	782.3	774.4	782.0	
	703.8	masked	703.6	
	566.9	513.9	557.5	
IV	3962.5		3962.5	HF
	3881.2		3881.2	$HF\cdots N_2$
	1404.6			HCF
	1305		1297	CH_4
	1278.8	1278.8	1248.6	CF
	1180.7	1182.9	1153.3	HCF
	1161.9, 1159.9	*1190.7*, 1188.5	*1139.5*, 1137.0	CH_2F
V	*2120.2*, 2102.3	*2120.2*, 2102.3	*2120.2*, 2102.3	A
	1960.3	1960.3	1960.3	B
	1942.4	1942.4	1942.4	A
	1854.7	1854.7	1854.7	A
	1709.5	1709.5	1709.5	C

[a] All frequencies are in cm^{-1}. Stronger absorptions are in italics.

variation in absorption intensity caused by UV (240 nm < λ < 380 nm) irradiation, despite the fact that the mercury arc lamp light intensity is much higher in the visible region. It is also notable that, while many product absorptions show dramatic changes in the course of photolysis, the absorptions at 783 and 707 cm^{-1} only gradually increase at first regardless of irradiation wavelength and later remain almost unchanged in further cycles of photolysis.

On the basis of the behaviors upon photolysis, annealing, isotopic substitution, and change in concentration, the product absorptions are sorted into five groups as listed in Table 1, and two of these are compared with the calculated frequencies in Tables 2 and 3. Group I absorptions are relatively weak in the original spectrum after the co-depositon of methyl fluoride and Ti atoms, but increase about 4 times upon UV irradiation. The Ti−H stretching absorptions in the region of 1580−1630 cm^{-1} shown in Figure 1 belong to this group. They increase and decrease repeatedly upon photolysis with UV (240 nm < λ < 380 nm) and visible (λ > 530) light, respectively, and they decrease gradually in the annealing cycles.

Group II absorptions are strong in the original spectrum after co-deposition, but decrease to about a third in intensity upon UV irradiation. They decrease and increase repeatedly upon irradiation cycles with UV and visible light, precisely the opposite of group I. Furthermore, group II absorptions triple in intensity upon annealing to 14, 20, and 26 K, as shown in Figure 4, and gradually decrease at higher temperature. No Ti−H stretching absorptions are included in this group. The distinct behaviors of groups I and II indicate that each group originates from a different reaction product, and the reaction products are interconvertible in such a manner that an increase in concentration of one product leads to a decrease in concentration of the other product.

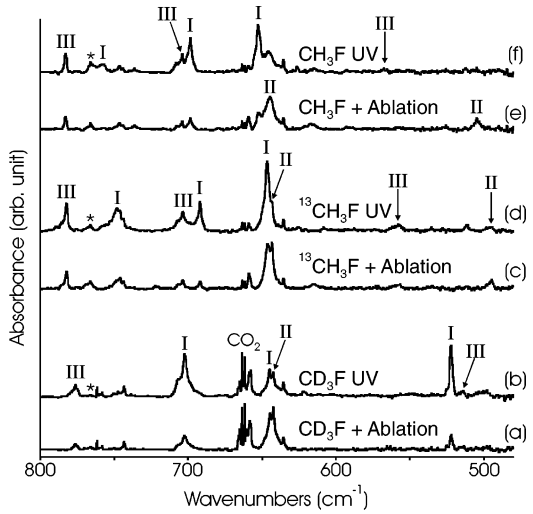

Figure 3. IR spectra in the region of 480−800 cm^{-1} for laser-ablated Ti atoms co-deposited with methyl fluoride isotopomers diluted in Ar at 7 K. (a) Ti + 0.2% CH_3F in Ar co-deposited for 1 h, (b) after broad-band photolysis with a UV transmitting filter (240 nm < λ < 380 nm) for 10 min, (c) Ti + 0.2% $^{13}CH_3F$ in Ar co-deposited for 1 h, (d) after broad-band photolysis with a UV transmitting filter (240 nm < λ < 380 nm) for 10 min, (e) Ti + 0.2% CD_3F in Ar co-deposited for 1 h, and (f) after broad-band photolysis with a UV transmitting filter (240 nm < λ < 380 nm) for 10 min. "I", "II", or "III" indicates the product band group. The absorption from TiN_2 is marked with "*".

Group III absorptions, including the absorptions at 703.8 and 782.3 cm^{-1}, are observed after co-deposition of methyl fluoride and laser-ablated Ti atoms. They grow gradually on photolysis, regardless of the wavelength, and later become constant. Once they grow, they never diminish in the following cycle of photolysis. On annealing, they grow considerably up to 35 K and sharpen, and their relative intensities increase at higher reagent concentration as shown in Figure 5.

Some of the product absorptions do not show particular changes on photolysis, and they are classed as group IV. These

TABLE 2: Observed and Calculated Fundamental Frequencies of CH_2=TiHF in the Ground Electronic State (^1A)[a]

	CH_2=TiHF				CD_2=TiDF			$^{13}CH_2$=TiHF		
description	obsd	calcd[b]	calcd[c]	int	obsd	calcd[c]	int	obsd	calcd[c]	int
ν_1 CH str		(3187.0)	3191.0	1		2362.8	2		3180.0	1
ν_2 CH str		(2854.8)	2879.1	5		2094.7	3		2872.6	5
ν_3 Ti−H str	1602.8	(1671.5)	1699.9	393	1158.6	1216.7	211	1602.8	1699.9	393
ν_4 CH_2 scis		(1329.1)	1325.6	25		1050.8	31		1315.5	24
ν_5 C−Ti str	757.8	(817.0)	818.5	125	644.9	697.9	43	748.4	806.6	149
ν_6 Ti−F str	698.6	(734.8)	747.9	151	702.6	742.1	184	692.0	742.1	126
ν_7 CH_2 wag	652.8	(693.3)	680.1	172	522.1	536.4	125	646.6	674.0	168
ν_8 CTiH bend		(606.8)	611.9	14		470.4	11		610.8	14
ν_9 CH_2 twist		(510.9)	492.2	25		351.1	9		492.2	25
ν_{10} CH_2 rock		(378.1)	357.7	4		295.9	3		353.7	5
ν_{11} CTiF bend		(186.3)	193.0	25		158.9	7		192.3	25
ν_{12} TiH OOP bend		(53.9)	95.4	156		77.1	102		95.3	155

[a] Frequencies and intensities are in cm^{-1} and km/mol. Intensities are SDD calculated values. [b] B3LYP/6-311+G(2d, p) for all atoms in parentheses. [c] B3LYP/6-311+G(2d, p)/SDD.

TABLE 3: Observed and Calculated Fundamental Frequencies of CH_3TiF in the Ground Electronic State (^3A)[a]

	CH_3-Ti-F				CD_3-Ti-F			$^{13}CH_3-Ti-F$		
description	obsd	calcd[b]	calcd[c]	int	obsd	calcd[c]	int	obsd	calcd[c]	int
ν_1 A′ CH_3 str		(3085.0)	3089.1	4		2281.0	1		3078.9	4
ν_2 A′ CH_3 str		(3028.2)	3027.2	6		2235.9	1		3016.9	6
ν_3 A′ CH_3 str		(2968.4)	2967.9	6		2129.6	1		2964.4	7
ν_4 A′ CH_3 def		(1427.8)	1428.2	4		1035.8	4		1425.0	4
ν_5 A′ CH_2 scis		(1419.1)	1420.1	1		1030.4	1		1417.0	1
ν_6 A′ CH_2 scis	1105.7	(1147.7)	1150.7	10	871.1	904.7	25	1096.9	1141.2	9
ν_7 A′ Ti−F str	646.3	(665.6)	678.1	183	642.3	676.4	174	643.3	678.0	183
ν_8 A′ C−Ti str	504.3	(530.4)	539.6	49	452.4	477.0	43	494.7	530.0	47
ν_9 A″ TiCH bend		(410.7)	414.7	19		329.0	11		409.7	20
ν_{10} A″ CH_3 rock		(405.2)	408.4	22		304.6	15		406.4	21
ν_{11} A″ CH_2 rock		(129.6)	134.2	5		125.1	5		133.2	5
ν_{12} A″ CTiF bend		(101.9)	98.8	1		74.7	2		98.7	0

[a] Frequencies and intensities are in cm^{-1} and km/mol. Intensities are SDD calculated values. [b] B3LYP/6-311+G(2d, p) for all atoms in parentheses. [c] B3LYP/6-311+G(2d, p)/SDD.

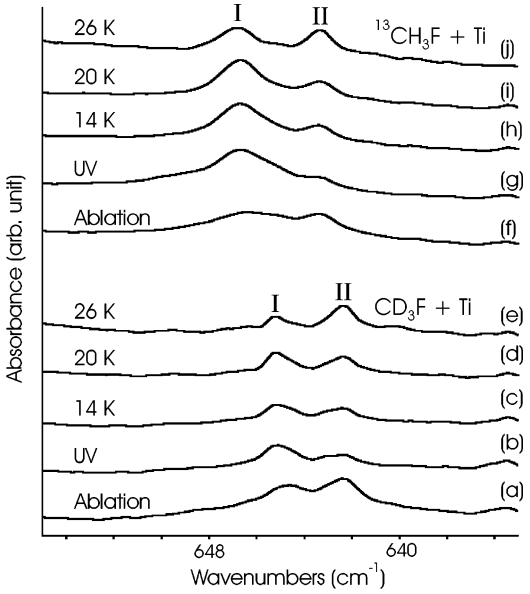

Figure 4. Annealing behavior for infrared spectra in the regions of 635−655 cm^{-1}. (a) Ti + 0.2% CD_3F in Ar co-deposited for 1 h, (b) after UV (240 nm < λ < 380 nm) irradiation for 10 min, (c) after annealing to 14 K, (d) after annealing to 20 K, and (e) after annealing to 26 K. (f) Ti + 0.2% $^{13}CH_3F$ in Ar co-deposited for 1 h, (g) after UV (240 nm < λ < 380 nm) irradiation for 10 min, (h) after annealing to 14 K, (i) after annealing to 20 K, and (j) after annealing to 26 K.

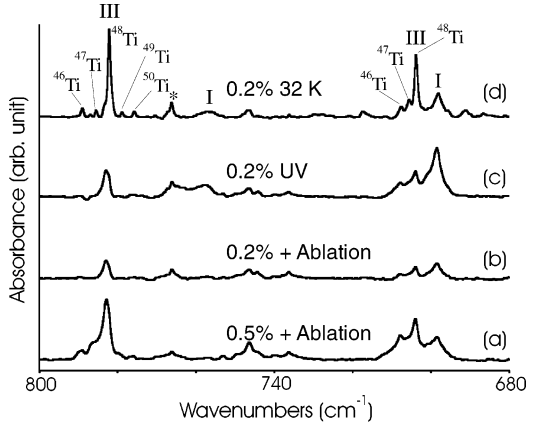

Figure 5. IR spectra in the region of 680−800 cm^{-1} for laser-ablated Ti atoms co-deposited with CH_3F diluted in Ar at 7 K. (a) Ti + 0.5% CH_3F in Ar co-deposited for 1 h, (b) Ti + 0.2% CH_3F in Ar co-deposited for 1 h, (c) after broad-band photolysis with a UV transmitting filter (240 nm < λ < 380 nm) for 10 min, and (d) after annealing to 32 K. "I" or "III" indicates the product band group. The absorption from TiN_2 is marked with "*".

are mostly fragments of methyl fluoride,[14] from interaction with high-energy radiation in the laser-ablation process. The frequencies of group IV absorptions are summarized in Table 1, and the strongest bands are shown in Figure 2. No absorptions are found for CH_3 or TiF products. Trace absorptions are observed for TiN_2 and TiO_2.[6,7]

Relatively sharp absorptions, group V, are observed in the region of 1690−2140 cm^{-1} as shown in Figure 6, an area clean in the spectrum of methyl fluoride. Importantly, these absorptions show no isotopic shifts. They are further sorted into three subgroups, A, B, and C. Subgroup A increases and decreases with UV (240 nm < λ < 380 nm) and with visible light (λ > 530 nm), respectively. Subgroup B also increases and decreases on UV and visible photolysis, respectively, but the variation in intensity is not as large as subgroup A, and subgroup B grows remarkably in the process of annealing. On the other hand, subgroup C decreases and increases on UV and visible photolysis, respectively, the reverse of subgroup A. Finally, no absorptions are observed at 3901 and 3913 cm^{-1} for the recently observed 1 $^3\Pi_u \leftarrow {}^3\Delta_g$ electronic transition of Ti_2.[30]

DFT calculations were performed for structures of formula $TiCH_3F$, and the ^1A methylidene and ^3A Grignard-type insertion product structures illustrated in Figure 7 are the most stable: CH_3TiF (^3A) is 22 kcal/mol lower in energy than $CH_2{=}TiHF$ (S), which exhibits significant α-agostic hydrogen interaction. A planar triplet methylidene with no α-agostic hydrogen interaction is 8 kcal/mol higher than the singlet, and a singlet CH_3TiF molecule with almost the same structure is 34 kcal/mol higher than the global minimum triplet. Table 4 compares calculated parameters for the observed CH_3-TiF and $CH_2{=}TiHF$ molecules, and Figure 7 illustrates their structures.

Transition state (TS) calculations on the triplet and singlet potential surfaces where performed using the QST2 option in Gaussian 98. We find a triplet transition state 38 kcal/mol higher than the CH_3TiF (T) global minimum: The triplet TS has one imaginary frequency, 638 cm^{-1} in a hydrogen diformation mode, a 1.989 Å Ti−C bond length, and 707 and 639 cm^{-1} Ti−C and Ti−F mixed mode frequencies. We note that these are intermediate between the analogous modes observed for the singlet methylidene (758 and 699 cm^{-1}) and the triplet CH_3TiF (646 and 504 cm^{-1}) and the calculated Ti−C bond lengths 1.812 and 2.101 Å (Table 4). Clearly α-hydrogen transfer is accompanied by a decrease in Ti−C bond length. The singlet TS has 2 kcal/mol higher energy than and similar structure to the triplet transition state, calculated Ti−C bond length 1.857 Å, and 976 cm^{-1} imaginary frequency. Figure 8 shows the relative

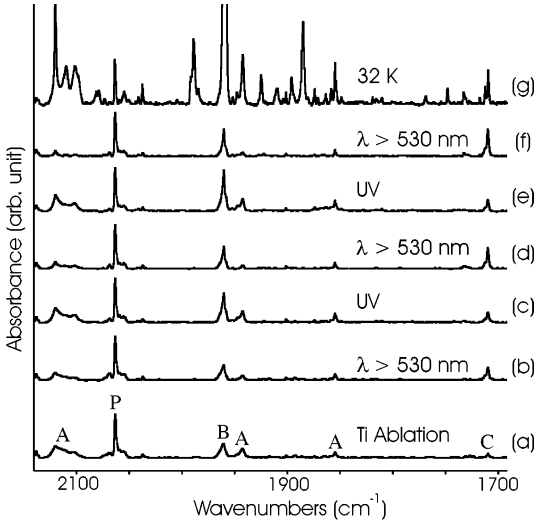

Figure 6. IR spectra in the region of 1690−2140 cm^{-1} for laser-ablated Ti atoms co-deposited with Ar/CH_3F at 7 K. (a) Ti + 0.2% CH_3F in Ar co-deposited for 1 h, (b) after broad-band photolysis with a filter (λ > 530 nm) for 30 min, (c) after broad-band photolysis with a UV transmitting filter (240 nm < λ < 380 nm) for 10 min, (d) after broad-band photolysis with a filter (λ > 530 nm) for 30 min, (e) after broad-band photolysis with a UV transmitting filter (240 nm < λ < 380 nm) for 10 min, (f) after broad-band photolysis with a filter (λ > 530 nm) for 60 min, and (g) after annealing to 32 K. The product absorptions are believe to arise from electronic transitions are marked with "A", "B", or "C" on the basis of the behaviors upon photolysis and annealing. "P" indicates precursor absorption.

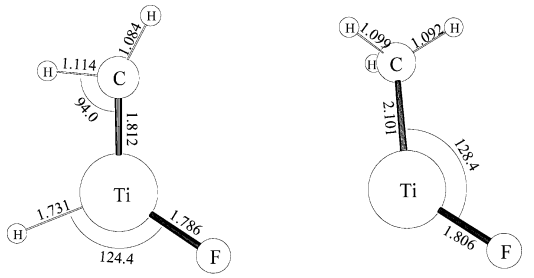

CH_2=TiHF (I) CH_3TiF (II)

Figure 7. Optimized molecular structures of Ti−methyl fluoride complexes identified in this study. The bond lengths and angles are in angstroms and degrees. The methylene group is noticeably distorted, and one of the methylene hydrogen atoms is very close to the Ti atom, indicating a strong agostic interaction between the atoms.

energies of Ti and CH_3F, both transition states, and the reaction products.

Calibration calculations were done for TiF. The ground state is $^4\Phi$ with 650.7 cm^{-1} fundamental frequency and 1.831 Å bond length.[31] Using B3LYP and the all-electron 6-311+G(2d,p) basis, we find a quartet state with $\langle s^2 \rangle = 3.750$, a 643 cm^{-1} harmonic frequency, and a 1.837 Å bond length. Higher level CCSD(T) calculations characterize the $^4\Phi$ ground state with $\langle s^2 \rangle = 3.753$, a 634 cm^{-1} harmonic frequency, and a 1.869 Å bond length.[32] Our DFT results are in excellent agreement with experiment and higher level calculations.

Group I. Group I absorptions are shown marked with "I" in Figures 1−3. The strong absorptions at 1602.8 and 1610.6 cm^{-1} with no ^{13}C shift and 1.383 H/D ratio are assigned to the Ti−H stretching mode of the reaction product as described above, indicating that C−H insertion by the metal atom readily occurs in the reaction of methyl fluoride with laser-ablated Ti atoms. A weak broad 1668 cm^{-1} absorption that tracks on irradiation but not annealing and shifts to 1205 cm^{-1} with CD_3F (also

TABLE 4: Geometric Parameters and Physical Constants Calculated for CH_2=TiHF and CH_3−TiF[a]

parameter	CH_2=TiHF	CH_3−TiF
r(C−H)	1.084, 1.114	1.092, 1.099, 1.099
r(C−Ti)	1.812	2.101
r(Ti−H)	1.731	
r(Ti−F)	1.786	1.806
∠HCH	114.2	107.7, 108.1, 108.1
∠CTiF	119.0	128.4
∠CTiH	111.7	
∠HTiF	124.4	
∠HCTi	94.0, 151.4	115.0, 108.8, 108.9
Φ(HCTiH)	158.8, −11.7	
Φ(HCTiF)	2.4, −168.1	0.3, 121.1, −121.8
mol sym	C_1	C_1
q(C)[b]	−0.61	0.73
q(H)[b,c]	−0.12, 0.10, 0.15	0.12, 0.12, 0.12
q(Ti)[b]	0.89	0.79
q(F)	−0.41	−0.43
μ[d]	1.60	2.62
state[e]	^{1}A	^{3}A
ΔE[f]	66	88

[a] B3LYP/6-311+G(2d,p)/SDD: bond lengths and angles are in Å and deg. [b] Mulliken atomic charge. [c] Numbers are in the order from the closest one to the metal atom to the farthest from. [d] Molecular dipole moment in D. [e] Electronic state. $\langle s^2 \rangle$ is 2.000 for ^{3}A after annihilation. [f] Binding energies in kcal/mol using the all-electron set for Ti are 72 and 92 kcal/mol, respectively.

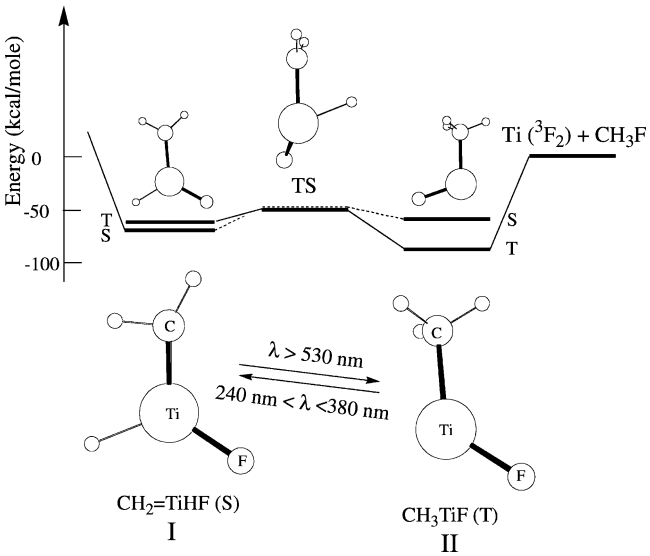

Figure 8. The photoreversible system identified in this study. CH_3-TiF is converted to CH_2=TiHF by UV (240 nm < λ < 380 nm) irradiation on the triplet surface followed by intersystem crossing, which is reversed by visible (λ > 530 nm) irradiation on the singlet surface followed by intersystem crossing. The higher energy singlet CH_3TiF, triplet transition state, and triplet CH_2=TiF structures are given above their energy levels.

labeled I in Figure 2) is due to a minor unidentified reaction product. Another strong absorption at 757.8 cm^{-1} shows isotope shifts of −9.0 and −112.9 cm^{-1} upon ^{13}C and D substitutions ($^{12}C/^{13}C$ and H/D isotopic frequency ratios of 1.012 and 1.175). Based upon the frequency, isotopic shifts, and DFT calculation results, the absorption is assigned to a mixed mode including the C−Ti stretching coordinate of the product. The frequency is higher than the expected C−Ti single bond stretching frequency (normally ∼500 cm^{-1}), which suggests that the bond between C and Ti is in fact a double bond, a point reinforced by the short computed C−Ti bond length (Figure 7).

The absorption at 698.6 cm^{-1} shows a small ^{13}C isotopic shift of −6.6 cm^{-1}, indicating that it probably arises from the mostly

Ti−F stretching mode of the product as Ti−F modes have been observed in this region.[31,33] The strong absorption at 652.8 cm^{-1} shows isotopic shifts of −4.9 and −135.4 cm^{-1} upon ^{13}C and D substitutions ($^{12}C/^{13}C$ and H/D isotopic ratios of 1.007 and 1.254), and probably originates from one of the CH_2 bending modes of the product. Consequently, the reaction product most likely contains Ti−H, C═Ti, CH_2, and Ti−F moieties, and the most probable compound that is consistent with the observed vibrational characteristics and also energetically favorable is CH_2═TiHF. The observed frequencies of group I absorptions compared with the DFT calculated values in Table 2 show very good agreement. The three lower frequencies are strongly mixed, which results in a positive CD_3 shift for the strong 702.6 cm^{-1} band of CD_2═TiDF. The four modes of CH_2═TiHF are predicted 4.3, 7.8, 5.2, and 6.2% higher using the all-electron basis.

Recently, the first transition-metal methylidene complex was formed from a simple halomethane in the reaction of methyl fluoride and laser-ablated Zr atoms and isolated in a solid argon matrix.[5] The present result indicates that a relatively small amount of CH_2═TiHF is produced in the reaction of methyl fluoride and Ti atoms, but the amount increases dramatically on UV photolysis through rearrangement from another reaction product. This also suggests that other transition-metal methylidene complexes can be produced by reaction of a halomethane and transition-metal atoms or photolysis afterward while trapped in an inert matrix. These methylidene complexes from a simple halomethane will eventually provide a new tool to study the nature of the high oxidation state transition-metal complexes including the effects of ligands and substituent modifications.

Group II. Figures 1−3 show that the compound responsible for group II is formed originally in a relatively large amount from reaction of methyl fluoride and Ti atoms in comparison with CH_2═TiHF. The strongest absorption of group II is observed at 646.3 cm^{-1} in the spectrum of Ti + CH_3F. This absorption shows small 3−4 cm^{-1} isotopic shifts on ^{13}C and D substitutions, which characterizes a predominantly Ti−F stretching mode. The weaker absorptions at 1105.7 and 1109.8 cm^{-1} show relatively small isotopic shifts of about −9 cm^{-1} and large shifts of about −240 cm^{-1} on ^{13}C and D substitutions ($^{12}C/^{13}C$ and H/D isotopic frequency ratios of 1.008 and 1.27), respectively. On the basis of the frequency and the isotopic shifts, they are attributed to a hydrogen deformation mode of the product split into two bands by the matrix. The absorptions at 504.3 and 507.9 cm^{-1} show isotopic shifts of −9.6 cm^{-1} and about −54 cm^{-1} on ^{13}C and D substitutions ($^{12}C/^{13}C$ and H/D isotopic ratios of 1.019 and 1.12), suggesting that they arise from the mostly Ti−CH_3 stretching mode of the product.

Like many other metal fluorides, the Ti−F stretching frequency of titanium fluorides generally increases with the number of Ti valence bonds.[31,33,34] The observed frequency, 646.3 cm^{-1}, is much lower than the previously observed antisymmetric frequencies of TiF_2 and TiF_3 at 740.6 and 792.8 cm^{-1} in an argon matrix,[33] but is rather close to the frequency of TiF at 650.7 cm^{-1} in the gas phase.[31] The present results indicate that the reaction product responsible for group II absorptions contains a −TiF moiety along with C−H and Ti−C bonds.

It is notable at this point that the most stable compound among the plausible reaction products is CH_3−TiF in its triplet ground state. It is straightforward to show in calculation that the approach of Ti atom to methyl fluoride on the side of fluorine eventually leads to the structure CH_3−TiF (T). Moreover, the predicted vibrational characteristics of CH_3−TiF (T) are in agreement with the observed values as shown in Table 3. The three modes are predicted 3.8, 3.0, and 5.2% too high using the all-electron basis set. The present results indicate that CH_3−TiF is readily generated in reaction of Ti atoms and methyl fluoride, and we expect that the reaction is promoted by excited Ti atoms produced in metastable states by laser ablation.[35] Furthermore, the extra electron density around fluorine appears to foster insertion by Ti as similar reactions with CH_4 gave weaker product spectra.

$$Ti(^3F_2) + CH_3F \rightarrow CH_3-TiF(^3A) \qquad (1)$$

The Photoreversible System. It is interesting, as in the reaction of methyl fluoride and laser-ablated Zr atoms,[5] that a transition-metal methylidene complex (CH_2═TiHF) is formed from methyl fluoride and laser-ablated Ti atoms, and that a photoreversible system is generated as well. However, unlike the zirconium study with intersystem crossing between the singlet and triplet states of CH_2═ZrHF, the present photoreversible system involves the methylidene complex (CH_2═TiHF) and the methyltitanium fluoride (CH_3−TiF) through α-hydrogen migration between carbon and titanium atoms. UV photolysis (240 nm < λ < 380 nm) transforms CH_3−TiF into CH_2═TiHF, whereas photolysis with visible light (λ > 530 nm) reverses this hydrogen-transfer process.

$$CH_3TiF\ (T) \xrightarrow{240>\lambda>380\ nm} CH_2{=}TiHF\ (T) \qquad (2a)$$

$$\Uparrow \qquad\qquad \Downarrow$$

$$CH_3TiF\ (S) \xleftarrow{\lambda>530\ nm} CH_2{=}TiHF\ (S) \qquad (2b)$$

The photoreversible CH_2═TiHF and CH_3−TiF system is illustrated in Figure 8, which involves intersystem crossings. Absorption in the UV initiates the α-H rearrangement on the triplet potential energy surface, reaction 2a, followed by intersystem crossing relaxation into the lower energy singlet state CH_2═TiHF (group I). Further visible irradiation promotes the S → S α-H restoration, reaction 2b, followed by relaxation to the global minimum triplet CH_3TiF (group II). In the reaction of methyl fluoride and laser-ablated Ti atoms, CH_3−TiF is originally generated much more than CH_2═TiHF, perhaps due to lower energy of the Grignard-type product. Upon irradiation by UV (240 nm < λ < 380 nm) light, CH_3−TiF is readily transformed via hydrogen migration into CH_2═TiHF, whereas reverse reaction occurs by visible (λ > 530 nm) irradiation. Finally, an increase in absorptions of CH_3−TiF with decrease in absorptions of CH_2═TiHF on annealing to 26 K is probably due to rearrangement of CH_2═TiHF to CH_3−TiF through hydrogen migration in the softer matrix cage owing to the stability of the Grignard-type product over the methylidene complex. Figure 4 shows these changes for $^{13}CH_3F$ and CD_3F reaction product spectra.

Agostic Interactions. The optimized geometries of CH_2═TiHF in its singlet ground and CH_3−TiF in the triplet ground states are illustrated in Figure 7, and the geometric parameters are summarized in Table 4. Both products have C_1 structures. The CH_3−TiF geometry is very close to a C_s structure, where C, Ti, F, and one of hydrogen atoms are in the same plane. However, the C_s structure is not an energy minimum, and the vibrational analysis gives an imaginary frequency for the HCTiF tortional mode. It is also noticeable in Figure 7 that one of the methylene hydrogen atoms is located unusually close to the Ti atom in the structure of CH_2═TiHF ($\angle$HCTi = 94.0° and r(Ti−H) = 2.192 Å), thus distorting the methylene group consider-

ably. Evidently there is strong agostic interaction between the metal atom and one of the α-hydrogen atoms in CH_2═TiHF.[36−39]

Agostic interactions have been found to be quite common, provided a metal has a low-lying empty valence orbital and a C−H bond in reasonable proximity. It is implicit that such a bond occurs always due to an attraction between the electron-deficient metal center and the C−H bond acting as a Lewis base. The interaction energy ranges between 10 and 15 kcal/mol, and as a result, the agostic bond often forms at the expense of a significant distortion within the ligand including bending at CH_2 and lengthening of the C−H bond. Therefore, the distorted structure of CH_2═TiHF is caused by the agostic interaction between the Ti atom and one of the α-hydrogen atoms.

Group III. Figure 5 shows IR spectra in the region of 680−800 cm^{-1} for Ti + CH_3F. Clearly the group III absorptions increase at high reagent concentration, on UV irradiation, and substantially on annealing relative to the group I absorptions. The absorption at 782.3 cm^{-1} shows an isotopic shift of 7.9 cm^{-1} on CD_3 substitution and an 0.3 cm^{-1} shift on ^{13}C substitution. The absorption at 703.8 cm^{-1} shows an isotopic shift of 0.2 cm^{-1} on ^{13}C substitution, and the corresponding absorption in the spectrum of Ti + CD_3F is masked by CD_2═TiDF. Based on these small isotopic shifts, both absorptions arise from vibrational modes where the F atom is heavily involved, such as Ti−F stretching modes of strong bonds, but C and H are coupled slightly.

The strong, sharp 782.3 cm^{-1} absorption (^{48}Ti) clearly shows natural abundance Ti isotopic splittings at 789.1, 785.6, 779.0, and 775.9 cm^{-1} for ^{46}Ti, ^{47}Ti, ^{49}Ti, and ^{50}Ti. These separations (3.1, 3.3, 3.3, and 3.5 cm^{-1}) are slightly larger than found for the $\nu_3(b_2)$ mode of TiO_2 (2.8−3.1 cm^{-1})[6] and are about the same as reported for TiF_3,[30] which suggests an antisymmetric Ti−F_2 vibration. The TiF_4 molecule is observed at 800 cm^{-1}, higher than TiF_3 at 793 cm^{-1} and TiF_2 at 741 cm^{-1}.[30,34] On the other hand, the two weak 707.6 and 705.6 cm^{-1} satellites on the associated stronger 703.8 cm^{-1} absorption show 2.0 and 1.8 cm^{-1} separation for these ^{46}Ti, ^{47}Ti, and ^{48}Ti absorptions. The smaller titanium isotopic separations are expected for the greater motion of F in a symmetric Ti−F_2 stretching mode as has been found for $\nu_1(a_1)$ of TiO_2.[6]

Weak absorptions at 1385.2 and 1378.4 cm^{-1} also track with the stronger group III bands. These bands show 3.3, 3.2 cm^{-1} ^{13}C shifts and a 374 cm^{-1} CD_3 shift, which are appropriate for a methyl group bending mode such as observed at 1462.4 cm^{-1} for CH_3F, 1460.4 cm^{-1} for $^{13}CH_3F$, and 1126.7 cm^{-1} for CD_3F. The 12/13 isotopic frequency ratios for group III and CH_3F are 1.0024 and 1.0014, respectively, and the CH_3/CD_3 frequency ratios are 1.370 and 1.300, respectively.

In the lower frequency region, a much weaker absorption is observed at 566.9 cm^{-1}, which shows a 9.4 cm^{-1} isotopic shift on ^{13}C substitution ($^{12}C/^{13}C$ isotopic frequency ratio 1.018) and a shift of 53 cm^{-1} on deuteration (CH_3/CD_3 isotopic frequency ratio of 1.103). These shifts are appropriate for a Ti−CH_3 stretching mode. The above considerations suggest that group III absorptions arise from the $(CH_3)_2TiF_2$ molecule.

The IR spectrum of $(CH_3)_2TiCl_2$ has been investigated, and the three strongest bands are 1375.5, 570.0, and 557.5 cm^{-1}.[10] The former antisymmetric CH_3 bending mode is a model for our 1385.2 cm^{-1} absorption. The 570.0 cm^{-1} antisymmetric Ti−Cl_2 mode must be increased for the lighter mass of fluorine, and 782.3 cm^{-1} is reasonable. The latter antisymmetric Ti−C_2 mode, which shifts 64 cm^{-1} on CD_3 substitution, is a model for our 567 cm^{-1} absorption. Unfortunately, the C−H stretching modes are masked by like CH_3F absorption. Our strongest two absorptions, at 782.3 and 703.8 cm^{-1}, are assigned on the basis of Ti, C, and D isotopic frequencies to antisymmetric and symmetric Ti−F_2 stretching modes in $(CH_3)_2TiF_2$.

Calculations were done for $(CH_3)_2TiF_2$ at the B3LYP/6-311+G(2d,p)/SDD level. The structure is in good agreement with that computed for the chlorine compound at the BP86 level.[40] We find Ti−C length 2.059 Å and C−Ti−C angle 105.3° as compared to 1.047 Å and 104.5° for the chlorine derivative. Our observed fundamentals for $(CH_3)_2TiF_2$ are in excellent agreement in frequency and relative intensity with the calculated values: 1423 cm^{-1} (14 km/mol), 797 cm^{-1} (235 km/mol), 719 cm^{-1} (165 km/mol), and 583 cm^{-1} (112 km/mol).

Group IV. The product absorptions whose intensities remain practically unchanged in the course of photolysis are sorted into group IV. Among them, the absorptions at 1162 and 1180 cm^{-1}, which arise from the C−F stretching modes of CH_2F and HCF, are the strongest as shown in Figure 2. The identified reaction products are consistent with those from vacuum UV photolysis of methyl fluoride as reported in a previous study by Jacox and Milligan.[14] This result suggests that the dissociation occurs through vacuum UV light emitted from the metal atoms in high-energy states during the laser-ablation process. Evidently the reaction products responsible for group IV absorptions, including radicals, do not affect the interconversions between CH_2═TiHF and CH_3−TiF in the photolysis cycles.

Group V. Group V absorptions are shown in Figure 6. These bands reveal no isotopic shifts on ^{13}C and D substitution. They also do not arise from any reaction product of Ti with O_2, N_2, or H_2,[6−8] or with pure Ti in solid argon,[30] and this region in the infrared spectrum of methyl fluoride is absorption free. Therefore, it is reasonable to presume that they arise from electronic transitions of Ti reaction products. The 3d orbitals are normally degenerate, but when the atom is bonded to an organic group, such as methyl group, the orbitals obviously split. If they also mix with some other orbitals as a result of bonding, there can be a nonzero transition moment. Particularly in the case of CH_3−TiF (T), which has only two bonds, there are two unpaired nonbonding d electrons, and the d orbitals are perturbed by a methyl group and a fluorine atom. Therefore, d−d excitations are possible in the complex. In this regard the $1\ ^3\Pi_u \leftarrow\ ^3\Delta_g$ absorption of Ti_2 has recently been observed near 4000 cm^{-1} in a solid argon matrix.[30]

To estimate the frequencies of possible electronic transitions in the infrared region, time-dependent (TD) DFT calculations[41] were carried out for CH_3−TiF and other plausible reaction products. The results show that when there are unpaired d electrons on Ti atom in the complexes, electronic transitions in the infrared region are possible in most cases. Particularly in the case of CH_3−TiF, the lowest d−d electronic transition energy is predicted at slightly over 2000 cm^{-1}. In consideration of further stabilization by the matrix, the predicted frequency is consistent with the observed values.

Among the subgroups of electronic transitions A, B, and C on the basis of the behaviors on photolysis and annealing, subgroup A increases and decreases upon irradiation with UV and visible light, similar to group I; however, they show relatively high intensities in the original spectrum after co-deposition of methyl fluoride and Ti atoms, unlike group I. On the other hand, subgroup C decreases and increases upon irradiation with UV and visible light, similar to group II absorptions. Subgroup B behaves similar to subgroup A, but the relative intensity variation is much smaller.

With the information obtained in this study, it is difficult to assign definitively the electronic absorptions to a specific reaction product. Subgroup C appears to be due to CH_3-TiF in a sharp, well-defined matrix trapping site. These bands decrease and increase on irradiation by UV and visible light along with group II vibrational absorptions. The A and B absorptions most likely originate from other minor reaction products that cannot be identified by the infrared spectrum. These observations open a new possibility of investigating d−d electronic transitions in the mid-infrared region, particularly for Ti complexes.

Conclusions

Reactions of laser-ablated Ti atoms with methyl fluoride in excess of argon have been carried out during condensation at 7 K. The product absorptions are sorted into five groups on the basis of the behaviors upon photolysis and annealing. Group I is weak after co-deposition of methyl fluoride and titanium atoms, but grows dramatically upon UV irradiation and then repeatedly decreases and increases following visible ($\lambda > 530$ nm) and UV (240 nm $< \lambda <$ 380 nm) irradiation cycles. Group II absorptions show the reverse trend. Spectroscopic evidence and DFT calculation results indicate that groups I and II arise from $CH_2{=}TiHF$ and a methyltitanium fluoride, CH_3-TiF, and they exhibit a persistent photoreversible system involving α-hydrogen migration. The molecular structure of $CH_2{=}TiHF$ shows evidence of α-agostic interaction between the metal atom and one of the α-hydrogen atoms in the ground singlet state.

Group III is identified as $(CH_3)_2TiF_2$, the result of spontaneous reaction of CH_3-TiF and CH_3F, whose absorption intensities become much stronger at higher reagent concentration and on annealing. Other reaction products are also identified mostly from vacuum UV photolysis of methyl fluoride. Interestingly enough, several electronic absorptions are also observed in the infrared spectrum, and they open a possibility of studying d−d transitions of alkylidene compounds in the infrared region. As shown in this study, transition-metal methylidenes can be readily formed by reaction of a halomethane and vaporized metal atoms, and these compounds show interesting photoreversibility phenomena.

Acknowledgment. We gratefully acknowledge financial support for this work from NSF Grant CHE 00-78836 and sabbatical leave support (H.-G. Cho) from the Korea Research Foundation (KRF-2003-013-C00044).

References and Notes

(1) Schrock, R. R. *Chem. Rev.* **2002**, *102*, 145.
(2) Buchmeiser, M. R. *Chem. Rev.* **2000**, *100*, 1565.
(3) (a) Legzdins, P.; Tran, E. *J. Am. Chem. Soc.* **1997**, *119*, 5071. (b) Choi, S.-H.; Lin, Z. *Organometallics* **1999**, *18*, 5488.
(4) Baumann, R.; Stumpf, R.; Davis, W. M.; Liang, L.-C.; Schrock, R. R. *J. Am. Chem. Soc.* **1999**, *121*, 7822.
(5) Cho, H.-G.; Andrews, L. *J. Am. Chem. Soc.* **2004**, in press.
(6) Chertihin, G. V.; Andrews, L. *J. Phys. Chem.* **1995**, *99*, 6356 (TiO_2).
(7) Chertihin, G. V.; Andrews, L. *J. Phys. Chem.* **1994**, *98*, 5891.
(8) Chertihin, G. V.; Andrews, L. *J. Am. Chem. Soc.* **1994**, *116*, 8322.
(9) Lee, Y. K.; Manceron, L.; Papai, I. *J. Phys. Chem. A* **1997**, *101*, 9650.
(10) McGrady, G. S.; Downs, A. J.; Bednall, N. C.; McKean, D. C.; Thiel, W.; Jonas, V.; Frenking, G.; Scherer, W. *J. Phys. Chem. A* **1997**, *101*, 1951, and references therein.
(11) (a) Franci, M. M.; Pietro, W. J.; Hout, R. F., Jr.; Hehre, W. J. *Organometallics* **1983**, *2*, 281. (b) Franci, M. M.; Pietro, W. J.; Hout, R. F., Jr.; Hehre, W. J. *Organometallics* **1983**, *2*, 815.
(12) Cundari, T. R.; Gordon, M. S. *J. Am. Chem. Soc.* **1992**, *114*, 539.
(13) Siegbahn, P. E. M.; Blomberg, M. R. A. *Organometallics* **1994**, *13*, 354.
(14) Jacox, M. E.; Milligan, D. E. *J. Chem. Phys.* **1969**, *50*, 3252.
(15) Raymond, J. I.; Andrews, L. *J. Phys. Chem.* **1971**, *75*, 3235.
(16) Andrews, L.; Miller, J. H.; Prochaska, E. S. *J. Am. Chem. Soc.* **1979**, *101*, 7158.
(17) Mucha, J. A.; Jennings, D. A.; Evenson, K. M.; Hougen, J. T. *J. Mol. Spectrosc.* **1977**, *68*, 122.
(18) Andrews, L.; Dyke, J. M.; Jonathan, N.; Keddar, N.; Morris, A.; Ridha, A *J. Phys. Chem.* **1984**, *88*, 2364.
(19) Lugez, C. L.; Forney, D.; Jacox, M. E.; Irikura, K. K. *J. Chem. Phys.* **1997**, *106*, 489.
(20) Nolte, J.; Wagner, H. Gg.; Sears, T. J.; Temps, F. *J. Mol. Spectrosc.* **1999**, *195*, 43.
(21) (a) Rosenman, E.; McKee, M. L. *J. Am. Chem. Soc.* **1997**, *119*, 9033. (b) Seccombe, D. P.; Tuckett, R. P.; Fisher, B. O. *J. Chem. Phys.* **2001**, *114*, 4074.
(22) Andrews, L.; Wang, X. *J. Phys. Chem. A* **2003**, *107*, 337.
(23) Cho, H.-G.; Andrews, L. *J. Phys. Chem. A* **2004**, *108*, 3965 ($Zr + C_2H_4$).
(24) Wang, X.; Andrews, L. Unpublished work from this laboratory.
(25) Burkholder, T. R.; Andrews, L. *J. Chem. Phys.* **1991**, *95*, 8697.
(26) Hassanzadeh, P.; Andrews, L. *J. Phys. Chem.* **1992**, *96*, 9177.
(27) Andrews, L.; Zhou, M.; Chertihin, G. V.; Bauschlicher, C. W., Jr. *J. Phys. Chem. A* **1999**, *103*, 6525.
(28) Zhou, M. F.; Andrews, L.; Bauschlicher, C. W., Jr. *Chem. Rev.* **2001**, *101*, 1931.
(29) Frisch, M. J.; Trucks, G. W.; Schlegel, H. B.; Scuseria, G. E.; Robb, M. A.; Cheeseman, J. R.; Zakrzewski, V. G.; Montgomery, J. A., Jr.; Stratmann, R. E.; Burant, J. C.; Dapprich, S.; Millam, J. M.; Daniels, A. D.; Kudin, K. N.; Strain, M. C.; Farkas, O.; Tomasi, J.; Barone, V.; Cossi, M.; Cammi, R.; Mennucci, B.; Pomelli, C.; Adamo, C.; Clifford, S.; Ochterski, J.; Petersson, G. A.; Ayala, P. Y.; Cui, Q.; Morokuma, K.; Rega, N.; Salvador, P.; DanneTierg, J. J.; Malick, D. K.; Rabuck, A. D.; Raghavachari, K.; Foresman, J. B.; Cioslowski, J.; Ortiz, J. V.; Baboul, A. G.; Stefanov, B. B.; Liu, G.; Liashenko, A.; Piskorz, P.; Komaromi, I.; Gomperts, R.; Martin, R. L.; Fox, D. J.; Keith, T.; Al-Laham, M. A.; Peng, C. Y.; Nanayakkara, A.; Challacombe, M.; Gill, P. M. W.; Johnson, B.; Chen, W.; Wong, M. W.; Andres, J. L.; Gonzalez, C.; Head-Gordon, M.; Replogle, E. S.; Pople, J. A. *Gaussian 98*, Revision A.11.4; Gaussian, Inc.: Pittsburgh, PA, 2002.
(30) Manceron, L. To be published (Ti_2).
(31) Ram, R. S.; Peers, J. R. D.; Teng, Y.; Adam, A. G.; Muntianu, A.; Bernath, P. F.; Davis, S. P. *J. Mol. Spectrosc.* **1997**, *184*, 186.
(32) Boldyrev, A. I.; Simons, J. *J. Mol. Spectrosc.* **1998**, *188*, 138.
(33) Hastie, J. W.; Hauge, R. H.; Margrave, J. L. *J. Chem. Phys.* **1969**, *51*, 2648.
(34) Beattie, I. R.; Jones, P. J. *J. Chem. Phys.* **1989**, *90*, 5209.
(35) A host of Ti* metastable states are observed below 2 eV: Moore, C. E. *Atomic Energy Levels*; National Bureau of Standards Circular 467; Washington, DC, 1952.
(36) Bau, R.; Mason, S. A.; Patrick, B. O.; Adams, C. S.; Sharp, W. B.; Legzdins, P. *Organometallics* **2001**, *20*, 4492.
(37) Wada, K.; Craig, B. Pamplin, C. B.; Legzdins, P.; Patrick, B. O.; Tsyba, I.; Bau, R. *J. Am. Chem. Soc.* **2003**, *125*, 7035.
(38) Ujaque, G.; Cooper, A. C.; Maseras, F.; Eisenstein, O.; Caulton, K. G. *J. Am. Chem. Soc.* **1998**, *120*, 361.
(39) Boncella, J. M.; Cajigal, M. L.; Abboud, K. A. *Organometallics* **1996**, *15*, 1905.
(40) Kaup, M. *Chem. Eur. J.* **1999**, *5*, 3631.
(41) Dattelbaum, D. M.; Omberg, K. M.; Hay, P. J.; Gebhart, N. L.; Martin, R. L.; Schoonover, J. R.; Meyer, T. J. *J. Phys. Chem. A* **2004**, *108*, 3527.